The Effects of Steady Magnetic Field on Solidification Microstructure and Distribution of Impurity Elements of Molten Carbon Steel

Haichuan Wang[1] Zhiyou Liao[1] Hui Kong[1] Wangsheng Zhang[2] Zhenxing Yin[1] and Shijun Wang[1]

[1]*School of Metallurgy & Resources, Anhui University of Technology(AHUT), Maanshan, 243002, China,*
[2]*Former Postgraduate of AHUT, Now Jiangxi Pingxiang Iron & Steel Corp., Pingxiang, 337019, China.*

(Received May 20, 2010; final form June 9, 2010)

ABSTRACT

Steady magnetic fields with different intensities were adopted to treat molten carbon steel. The refinement of crystal particles was tested, on which the magnetic field intensity was optimized. Original Position Analysis (OPA) technology was used to analyze the migration of impurity elements as well as the distribution and segregation of impurity elements P, S and C in the solidification process of molten carbon steel. Combined with the previous achievements, the effects of magnetic field on molten carbon steel have been discussed.

Keywords: magnetic field; molten carbon steel; solidification microstructure; impurity elements; distribution; segregation.

* Coresponding author. Tel: +86-555-2311043
E-mail : which@ahut.edu.cn (Haichuan Wang)

1. INTRODUCTION

The main applications of a steady magnetic field, especially one less than 1 tésla (T), are to stir metal melt, break up the dendrite, refine crystal particles and improve the quality and performance of steel /1,2/. Nowadays, researchers' attentions to the effects of magnetic field have been diverted from the refinement of crystal particles to the distribution of elements in the solidification process /3,4/. In recent researches, scholars conducted such studies of magnetic fields to treat alloys /5-13/. However they mainly focused on low melting point alloys instead of high melting point metals such as liquid iron and molten steel. In this article, magnetic field with intensity of 0~1 T was used to deal with molten carbon steel during its solidification process. The Original Position Analysis (OPA) technology was performed to quantitatively analyze the distribution of impurity elements P, S and C in steel ingot. The effects of steady magnetic field on the distribution of impurity elements are discussed.

2. EXPERIMENTAL PROCEDURE

Carbon steel was used as an experimental material. The samples were melted at 1823 K (1550°C) and the magnetic fields with different intensities were applied to the molten steels from the beginning of solidification (the schematic diagram of steady magnetic field is shown in **Figure 1**) to the end of cooling. The experimental results were analyzed and compared, the distribution of impurities elements in solidification microstructure were obtained. Details about the experiments are listed in **Table 1**.

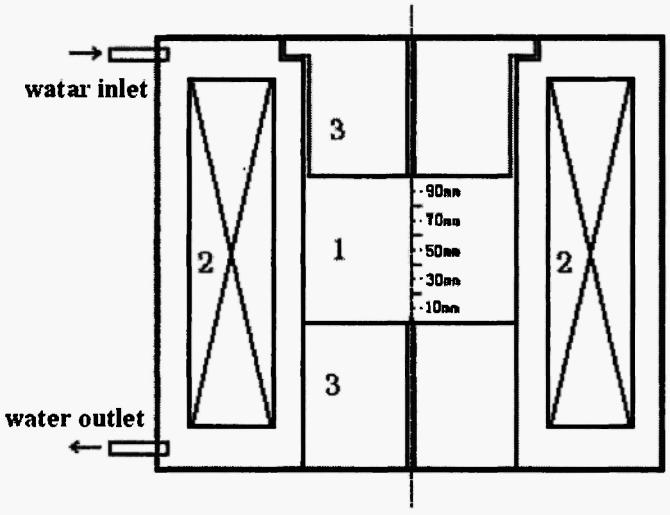

Fig. 1: Schematic diagram of steady magnetic field
1.The cavity of the magnetic field, 2. The loop of the magnetic field, 3. Pure iron for confining magnetic field

Table 1
The experimental arrangement for molten carbon steel processed by steady magnetic field

No.	1#	2#	3#	4#	5#
Current/A	0	5	10	15	20
Magnetic field/T	0	0.25	0.47	0.64	0.80
Treating time/min	0	120	120	120	120

3. RESULTS AND DISCUSSION

3.1 The Effects of Magnetic field on the Grain Refinement

The samples treated respectively with the steady magnetic fields (0, 0.25, 0.47, 0.64, 0.8T) were polished and corroded, then observed by an optical microscope (×100). Photographs of the solidified microstructure taken by a Panasonic WV-CP240 color digital camera are shown in **Figure 2**. Typical photographs of each sample were analyzed, the average number and size of crystal grains were determined by an image processing software (ImageJ). The statistical average values are shown in **Figure 3**.

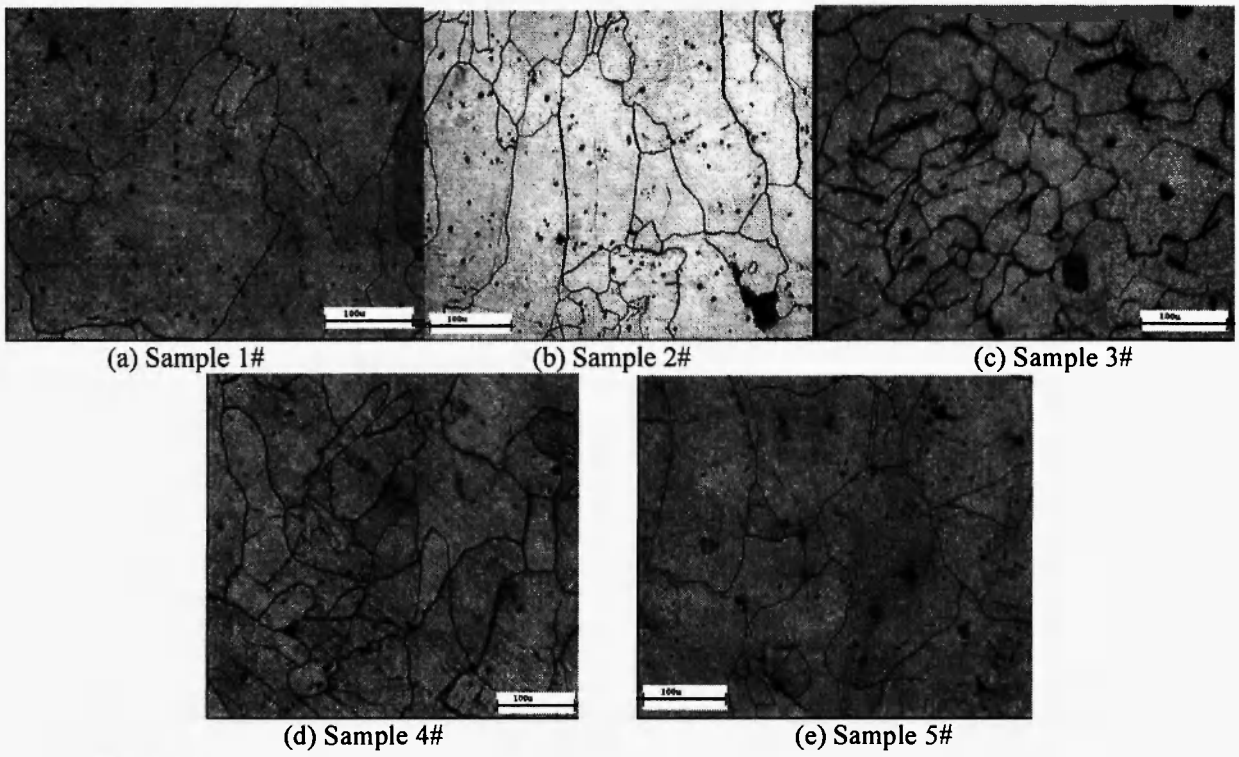

Fig. 2: Metallographic photographs of steel samples processed by high magnetic field (×100)

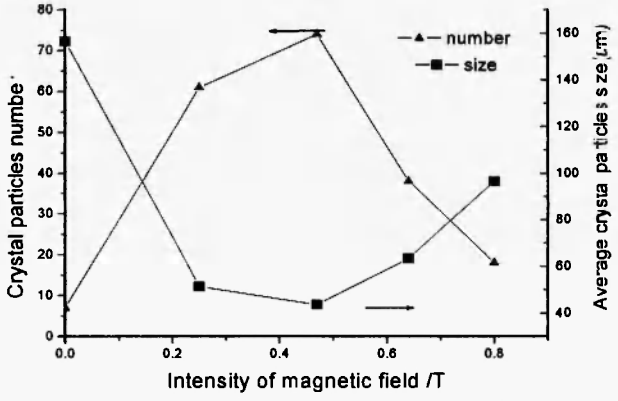

Fig. 3: The relationship between crystal grain number, size and intensity of the magnetic field

As shown in **Figure 2** and **Figure 3**, in the steel sample without magnetic fields processing, there are fewer total number of crystal grains, the crystal grain is relatively large and the average area of the crystal grain is the largest. Furthermore, the arrangement of crystal grains has no obvious direction. In the steel sample processed in a magnetic field of 0.25T, the crystal grains are obviously refined, the effects of the magnetic field on the solidification process and microstructure of steel are obvious. Although the crystal grains are still relatively large, they are smaller than the crystal grains in the sample without magnetic field processing, and the

columnar grains are further developed. After being processed in a magnetic field of 0.47T, the crystal grains are obviously smaller than those processed by 0.25T. In addition, the number of crystal grains increases, the average area of crystal grain and the columnar grain decreases, and a small equiaxed grain appears. As shown in **Figure 3**, the best refinement effect is obtained in 0.47T—when the magnetic field is more than 0.47T, the size of crystal grain becomes big, and the refinement effect reduces.

According to theoretical analysis, steady magnetic fields have an impact on crystal homogeneous nucleation, and the conduction imposed on the solidification process by the magnetic field could increase the overcooling degree of melt and promote a raise in the nucleation rate. Thermodynamic theory indicates that the standard Gibbs free energy of the solid-liquid phase per unit volume will change under a high magnetic field due to the impact of magnetic energy. The absolute value of Gibbs free energy in a system will enlarge under the high magnetic field. Therefore the magnetic energy produced from molten carbon steel being placed in magnetic field will promote nucleation. This is confirmed by experimentation in this study. The experimental results show that the higher magnetic strength can't bring better refinement. So the effects of a magnetic field on a solidification system are interpreted not only by thermodynamic conditions, but also by the kinetic conditions which affect the nucleation. When the electromagnetic force produced in the magnetic field hinders the flow of molten steel and inhibits the natural convection of melt, it promotes the nuclei growing upward and produces slightly more coarse crystal grains.

3.2 2D and 3D distribution of element C

The experimental samples were polished, then scanned and analyzed by the OPA technology in their bottom areas. The specification of the scanned samples was φ45mm × 10mm, the scanned area was 18mm × 18mm. These analyzed elements and their wavelength are 193nm for element C, 178.3nm for element P and 180.7nm for element S, respectively. The wavelength of compared element Fe is 187.7nm.

The distribution and segregation of the main elements in the solidification structure are obtained and shown in **Figure 4** to **Figure 6**. The 2D and 3D distribution of element C is shown in **Figure 4a** and **Figure 4b**, respectively.

Fig. 4a: 2-dimensional diagrams of content distribution of element C (Sample processed by 0.25T in left and 0.8T in right)

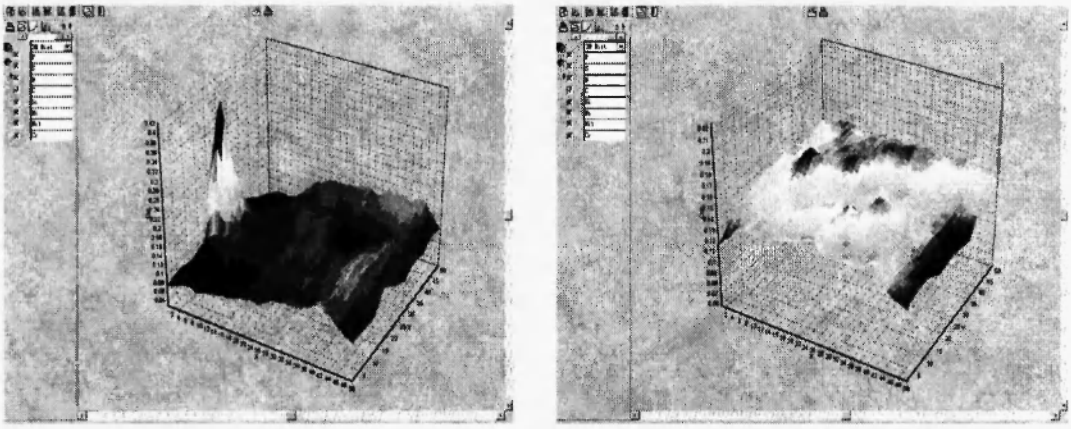

Fig. 4b: 3-dimensional diagrams of content distribution of element C
(Sample processed by 0.25T in left and 0.8T in right)

As shown in **Figure 4a**, the segregation degree of element C processed by 0.8T is smaller than that processed by 0.25T, and the distribution of element C presents uniform. Comparing the segregation degree of element C with its average content in the scanning region, though the original composition of the materials used in the experiments are the same, the OPA analysis shows that the average content of element w[C] is 0.124% at the bottom of the sample processed by magnetic field of 0.25T and 0.141% at the bottom of the sample processed by 0.8T. This shows that the average amount of element C increases at the bottom region of the sample when the magnetic field intensity increases, but the change tends to increase uniformly, and the amount of increase reduces when the magnetic field intensity increases. **Figure 4b** shows that, with the increasing of magnetic field intensity, the pinnacle of element C vanishes and negative segregation changes at the bottom of the sample.

3.3 2D and 3D distribution of element P

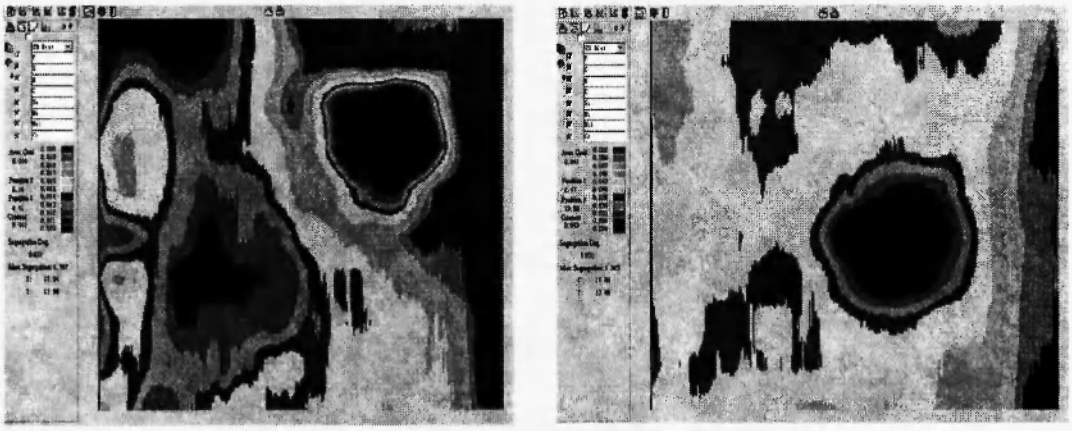

Fig. 5a: 2-dimensional diagrams of content distribution of P element
(Sample processed by 0.25T in left and 0.80T in right)

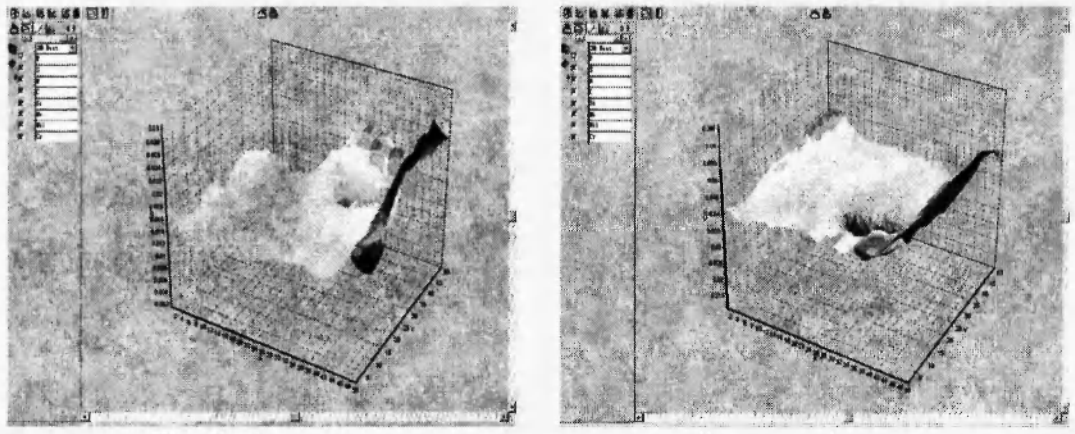

Fig. 5b: 3-dimensional diagrams of content distribution of element P (Sample processed by 0.25T in left and 0.8T in right)

Figure 5a shows that the segregation of element P is very serious and reflects polarization. There is a serious positive segregation in the vicinity of shrinkage, while there is negative segregation in other scanning regions, and a progressive wave-like content changes from left to right as shown in **Figure 5b**. Also from **Figure 5**, the average levels of element P at the bottom of the sample increases from 0.016% to 0.041% with the increasing of magnetic field intensity. This distribution of average content is extremely uneven and the large amount of positive segregation points leads to an increase in the average content.

3.4 2D and 3D distribution of element S

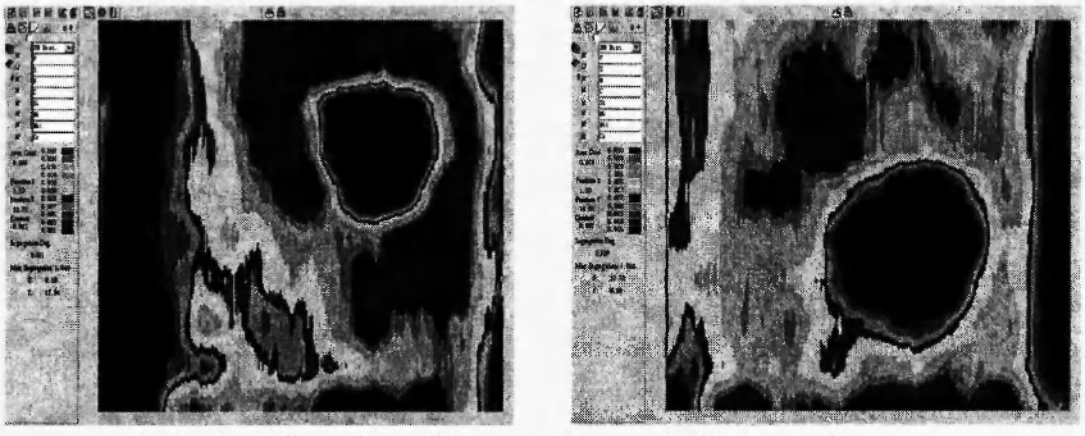

Fig. 6a: 2-dimensional diagrams of content distribution of element S (Sample processed by 0.25T in left and 0.8T in right)

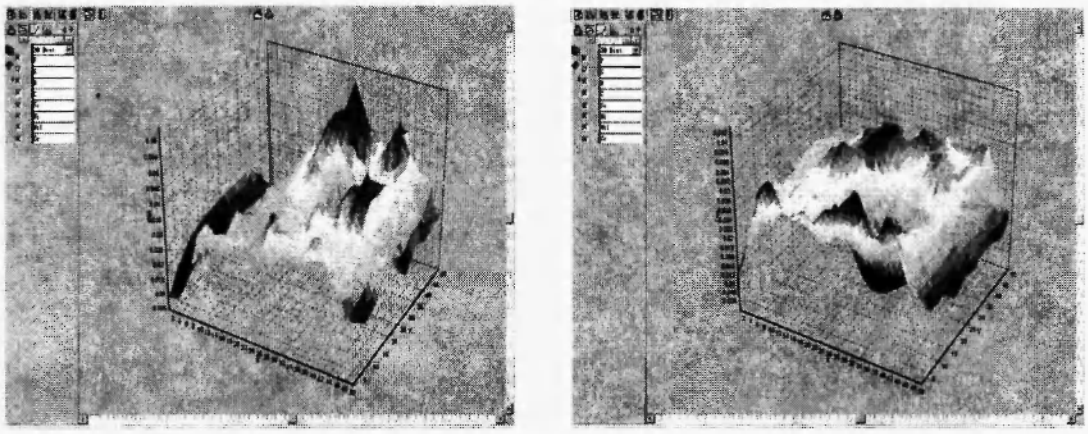

Fig. 6b: 3-dimensional diagrams of content distribution of element S
(Sample processed by 0.25T in left and 0.8T in right)

As shown in **Figure 6a**, there is a positive segregation band of element S in the center region, while there is a negative segregation band on the both sides of the positive segregation band. The span of the segregation bands is bigger, and the largest segregation degree is 1.940, which is more serious. As shown in **Figure 6**, after being processed by a magnetic field of 0.25T, the average content of element w[S] is 0.31%, it is the highest in the center of the sample, and the distribution of S content is extremely uneven—a peak-shape distribution appears in **Figure 6b**. The average content of S reaches a minimum of 0.024% in the scanning center for the sample processed by 0.8T, the peak-shape compresses, and the distribution of the average levels is still uneven.

3.5 The impact of magnetic field induce the element content at the bottom center of the samples change

The samples processed by magnetic fields of 0.25T and 0.8T were analysed respectively by OPA, the corresponding data are shown in **Table 2**.

Table 2
The average content and segregation of impurity elements P, S and C in the center area of samples

Element	2# (0.25T)		5# (0.8T)	
	Average Centre content/%	95% believe space/%	Average Centre content/%	95% believe space/%
C	0.124	[0.084 , 0.169]	0.141	[0.126 , 0.157]
P	0.016	[0.008 , 0.025]	0.041	[0.030 , 0.052]
S	0.031	[0.016 , 0.051]	0.024	[0.011 , 0.034]

As shown in **Table 2**, even though the original components of the samples are the same, the distribution of carbon increases and the average level of element C, P and S in center area of samples increases subsequently with the increasing of magnetic field intensity, but the degree of the increase is not very high. The increase in distribution of element P is linear—the distribution of P at the center site in samples rises, but the increasing trend is not large for element P which is related to the nature of element itself. The distribution of element S is contrary to element P—the average content of regional center in samples decreases, it is because of the decrease of melt surface free energy under the action of magnetic field. With the increasing

of magnetic field intensity, the average contents of element C, P and S in the regional center of the samples decrease. Element S is a surfactant element, it is easy to be enriched in the surface of solidification microstructure, which leads to a concentration decrease of S in the regional center.

4. CONCLUSION

This experiments show that when the magnetic field intensity reaches 0.47T, the level of crystal grain refinement is best. A magnetic field of over 0.47T reduce refinement, which confirms that the effects of steady magnetic field on crystal grain refinement exert a suitable intensity. Thermodynamic and kinetic properties must be considered simultaneously so that these optimal control parameters can be obtained.

The 2D and 3D distribution of elements shows that, with an increasing of magnetic field intensity (<1T): (1) The distributions of elements in the 3D map develop a certain formation at the bottom of the sample, and the peak point decreases; (2) The average content of C and P increases but the amount of element S decreases at the bottom of the sample. The OPA results show that the amount of element C and P in regional center of the sample increases with the increasing of magnetic field intensity, and the trend presents linear, while element S changes on the contrary because S has a different magnetic phenomenon.

ACKNOWLEDGEMENTS

The authors wish to express their appreciation to NSFC-Baosteel Unite Research Foundation (No.50774108) and Anhui Province Foundation of Science and Technology for Excellent Youth (No. 02041930) for their financial support.

REFERENCES:

1. Y. L. He, Y.S. Yang and Z.Q. Hu, *Materials Review,* **7**, 3-7 (2000). (in Chinese)
2. B. T Zi, W.J. Liu, K.F. Yao and J.Z. Cui, *Tianjin Metallurgy*, **5**, 5-8 (2002). (in Chinese)
3. Q. Wang, X.J. Pang, C.J. Wang, T. Liu, D. G. Li and J.C. He. *The 5th International Symposium on Electromagnetic Processing of Materials*, Sendai, Japan, ISIJ, Tokyo, (2006), p.387-390.
4. F. Yves, *The 5th International Symposium on Electromagnetic Processing of Materials*, Sendai, Japan, ISIJ, Tokyo, (2006), p.9-14.
5. S.M. Xing, Y.R. Xu, H.Q. Hu and B.S. Liu, *Special Casting & Nonferrous Alloys,* **6**, 38-40 (1998). (in Chinese)
6. T A. Bassyouni, Light Metal, 12, 733-742 (1983).
7. H. Yasuda, I. Ohnaka, O. Kawakami, K. Ueno and K. Kishio, *ISIJ International,* **43**, 942-949 (2003).
8. J.L. Wang, H. S. Di, X. M. Zhang, G.D. Wang and X.H. Liu, *Research on Iron and Steel*, 6, 37-40 (2001). (in Chinese)
9. Enomoto, T. Sonoyama and H. Yada, *Materials Transactions, JIM*, **1**, 189-195(1998).
10. V. M. Khlestov, E. V. Konopleva and H. J. Mcqueen, *Canadian Metallurgical Quarterly*, **2**, 75-89 (1998).
11. P. D. Hodgson, M.R. Hickson and R.K. Gibbs, *Scripta Materialia,* **10,** 1179-1184 (1999).
12. S. Michio, Y. Maruta and Y. Ysasunori, *CAMP-ISIJ*, **1**, 126 (1998).
13. X. Li, Z.M. Ren, H. Wang, W.X. Li, K. Deng, and Y.Q. Zhang, *Acta Metallurgica Sinica,* **1**, 40-45 (2004). (in Chinese)